Mechanism and electric field induced modification of magnetic exchange stiffness in transition metal thin films on MgO(001)

Abdul-Muizz Pradipto,[1,2,*] Toru Akiyama,[2] Tomonori Ito,[2] and Kohji Nakamura[2,3]

[1]*Institute for Chemical Research, Kyoto University, Uji, Kyoto 611-0011, Japan*

[2]*Department of Physics Engineering, Mie University, Tsu, Mie 514-8507, Japan*

[3]*Center for Spintronics Research Network, Graduate School of Engineering Science, Osaka University, Toyonaka, Osaka 560-8531, Japan*

(Received 12 February 2017; revised manuscript received 22 June 2017; published 18 July 2017)

Magnetic exchange stiffness in TM/MgO(001) [transition metal (TM) = Fe, Co, and Ni] is investigated by means of the first-principles full-potential linearized augmented plane wave method. We find that while the exchange stiffness constants are positive (ferromagnetic) in all considered systems, there are negative energy orbital contributions to the exchange stiffness preferring antiferromagnetic alignment. The different contributions can be explained simply in terms of bandwidth narrowing of the d_{xz} band arising from an introduction of spin canting on neighboring TM atoms along the x direction. This scenario reflects well the stability of the d bands, especially in the cases of Fe/MgO and Co/MgO, on going from the ferromagnetic state towards the spin spiral states, and the exchange stiffness constant may be determined by the position of the Fermi level. As for the Ni/MgO system, we find that the exchange stiffness constant is much smaller than in the other two cases due to the almost full occupation of the relevant d orbitals. When this mechanism which is associated with the bandwidth narrowing is applied to investigate the effect of external field on the exchange stiffness, we find that in both Fe/MgO and Co/MgO, the application of positive field increases the exchange stiffness due to the modification of the TM-O atomic distance.

DOI: 10.1103/PhysRevB.96.014425

I. INTRODUCTION

In the search for optimal realization for magnetic tunnel junction devices in spintronics technology [1–4], the control of magnetic properties via an application of electric voltage has received much attention for the last two decades [5–14]. Various properties which are known to be modified by an electric field include the magnetocrystalline anisotropy [7,8,15], magnetic coercivity [7,16], and the Curie temperature [5,17,18]. Other important properties, less explored in relation to the electric field effects, are the antisymmetric exchange (stiffness) interaction and the symmetric counterpart. The former stiffness involves spin-orbit coupling (SOC) and is associated with the Dzyaloshinskii-Moriya-like interaction (DMI) preferring perpendicular spin alignments on neighboring atomic sites [19–22]. The latter one, i.e., the symmetric exchange stiffness, is analogous to the isotropic exchange interactions in local magnets preferring parallel or antiparallel spin alignment. These exchange stiffnesses are technologically important as they, in addition to the magnetocrystalline anisotropy, may give rise to certain spin textures, such as the skyrmions [23], and since they determine the structure and dynamics of the homogenously magnetized regions or the magnetic domains [24,25]. Attempts to electrically control interfacial magnetic domain structures have just started rather recently, and systems where such investigations have been conducted have been rather limited to the CoFe/MgO- and Pt/Co-based interfaces [11–14].

Recent developments in magnetic measurement techniques [26–31] have opened the path on investigating the manipulation of the domain structures. A change in the domain structure does not straightforwardly imply modifications to the exchange stiffness, but it contains also the important contribution from the magnetic anisotropy [24,25] which is well known to be affected by external perturbations such as applied voltage. However, very recent magneto-optical Kerr (MOKE) spectroscopy measurements have revealed possible modifications to the exchange stiffness in Co/Pt [13] and MgO/CoFeB [14] interfaces. In the Co/Pt system, the change of the domain structure size due to an applied voltage far exceeds the expected modification due to only the anisotropy constant [13], suggesting that a more significant contribution comes from the exchange stiffness. The authors further predicted that the enhancement of the latter interaction strength is due to an increase of charge accumulation at the surface of Co for the Co/Pt system [13]. A similar observation is reported for the MgO/CoFeB interface, in which the increase of electron density at the CoFeB side due to a positive gate voltage is suggested to have increased the domain width [14]. The change in the domain width in the latter system is again more likely attributed to the modification of exchange stiffness. Despite the presence of these experimental indications, theoretical investigations of the electric field effects on the exchange stiffness, which can be expected to reveal the origin of the modulation, seem to date to be lacking, to the best of our knowledge. Such analysis constitutes the purpose of the present study.

In the present work, the mechanism of exchange stiffness and the effects of applying electric fields to the exchange stiffness constant are systematically investigated by first-principles density functional theory (DFT) calculations. For prototypical interfaces, we have chosen Fe/MgO and Co/MgO interfaces in which the contribution of the antisymmetric exchange stiffness or the Dzyaloshinskii-Moriya interaction to the exchange stiffness can be safely ignored in the first approximation, and focused more on the symmetric part. As will be shown shortly, such approximation is not very severe

*a.m.t.pradipto@gmail.com

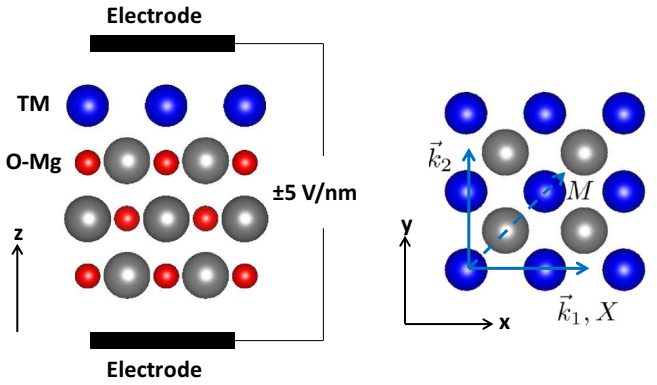

FIG. 1. Model structure used in calculations from the side (left) and top (right) views. In the side view, large (blue) spheres on the top denote transition metals (TM=Fe or Co), and small (red) and large (gray) spheres in the three bottom layers denote O and Mg atomic species, respectively. In the top view, only the TM and top layer of the Mg are visible, since the O atoms are situated at the bottom of the TM atoms.

and indeed the DMI is insignificant in these interfaces. This work is expected to shed more light on the origin of electric field induced modifications of the domain structures in metallic interfaces.

II. COMPUTATIONAL DETAILS

A slab consisting of a single layer of Fe or Co on top of three MgO(001) layers, as shown in Fig. 1, is employed. All calculations have been performed by using the generalized gradient approximation (GGA) [32] to the DFT as implemented in the full-potential linearized augmented plane wave (FLAPW) code [33–35]. Due to the absence of periodicity along the surface normal direction of the slab geometry, this method allows natural inclusion of external electric field. We apply gate voltages corresponding to the incorporation of homogenous electric fields of ±5 V/nm, and the direction has been chosen such that positive (negative) electric field refers to the application of positive (negative) gate voltage at the vacuum region of the Fe or Co side. A plane-wave cutoff $|\mathbf{k}+\mathbf{G}|$ of 3.9 a.u.$^{-1}$ has been chosen, and suitable muffin-tin radii of 2.2 bohrs have been used for both Fe and Co, and 2.0 and 1.4 bohrs for Mg and O, respectively. The in-plane lattice constant a has been fixed to the optimal parameter of cubic MgO, and the out-of-plane atomic positions are relaxed for each of the applied fields.

In this work, to compute the exchange stiffness constants $\mathcal{A}$, we start from ferromagnetic configurations, which are confirmed to be the ground state for all structures, in the scalar relativistic approximation, i.e., excluding spin-orbit coupling (SOC). Next we build a set of spin spiral structures having wave vectors $q = a/\lambda$ along the x direction by employing the generalized Bloch theorem [36,37], where λ is the wavelength of the spin spiral structures. Using this notation, $q = 0$ and $q = 0.5$ would respectively describe simple ferromagnetic and antiferromagnetic alignments. We consider sufficiently large 90×90 special k points in the chemical Brillouin zone for the spiral structure calculations to reduce numerical errors. Finally, the frozen magnon energy, $E(q)$, has been fitted with a polynomial, $E(q) = C_0 + C_2q^2 + C_4q^4$, where the odd terms with respect to the q drop due to the absence of SOC [38,39]. The C_2 is the exchange stiffness constant, and the C_4 is a higher order correction to this symmetric term which is not crucial at very small q. In order to check to effect of SOC, we have subsequently included SOC for supercells with lattice constants corresponding to wavelengths of the commensurate spin-spiral structures [40,41] in a non-self-consistent manner to reduce the computational costs. A Néel out-of-plane type rotation has been considered, in which the normal of the spin rotation plane is perpendicular both to the direction of the spin wave vector q and to the normal to the film plane along the z direction. Although the degeneracy of the $-q$ and q states is lifted, showing that asymmetric DMI has been induced by the SOC, the energetic difference between $q = \pm 0.1$ states is found to be on the order of 10^{-2} meV, indicating the insignificance of the DMI compared to symmetric part. We will therefore only discuss the non-spin-orbit-related exchange stiffness.

III. RESULTS AND DISCUSSION

We start by presenting the results of Fe/MgO at zero field. The calculated frozen magnon energy, $\Delta E(q)$, defined as the energy difference of the spin-spiral structures with q relative to the ferromagnetic state ($q = 0$) as a function of q, is shown in Fig. 2(a). It is obvious that a ferromagnetic state is the ground state and that the energy dispersion around $q = 0$ follows almost quadratic behavior. By fitting the $\Delta E(q)$ around $q = 0$, i.e., with $q = 0$, ± 0.02, ± 0.05, ± 0.1, and ± 0.2, we obtain an exchange stiffness constant of 217.5 meV Å^2. A direct comparison with exchange interaction in related systems, such as in bulk Fe [42], is not straightforward due to the reduced dimensionality in the present system. While our calculated value compares very well with previously estimated exchange stiffness in an unsupported Fe monolayer of 210 meV Å^2 [43], thicker iron films have a considerably larger exchange stiffness constant of 260 meV Å^2 [44].

We further estimate the orbital energy contributions to the exchange stiffness in the basis of energy density $\Delta E_n(q)$ defined as

$$\Delta E_n(q) = \int_{-\infty}^{\varepsilon_F} \varepsilon N_n(\varepsilon,q)d\varepsilon - \int_{-\infty}^{\varepsilon_F} \varepsilon N_n(\varepsilon,0)d\varepsilon, \quad (1)$$

where N_n is the density of states (DOS) projected to the Fe d_n ($n = d_{z^2}$, d_{xz}, d_{yz}, d_{xy}, and $d_{x^2-u^2}$) orbitals. The results are summarized in the inset of Fig. 2(a). It is interesting to note that the exchange stiffness results from competitions between strong ferromagnetic (positive) and antiferromagnetic (negative) energy contributions coming from different orbitals. Such competitions have been anticipated previously [42]. At $q = \pm 0.1$, for example, while the total exchange energy is 10.5 meV, the d_{xz} and d_{xy} orbitals give large positive energy contributions of 43.9 meV and 41.4 meV, respectively. On the other hand, the d_{yz} orbital has a very strong antiferromagnetic energy contribution of −66.5 meV. The d_{xz} and d_{yz} orbitals are degenerate in the collinear ferromagnetic state, $q = 0$, that holds fourfold symmetry. This degeneracy is then removed

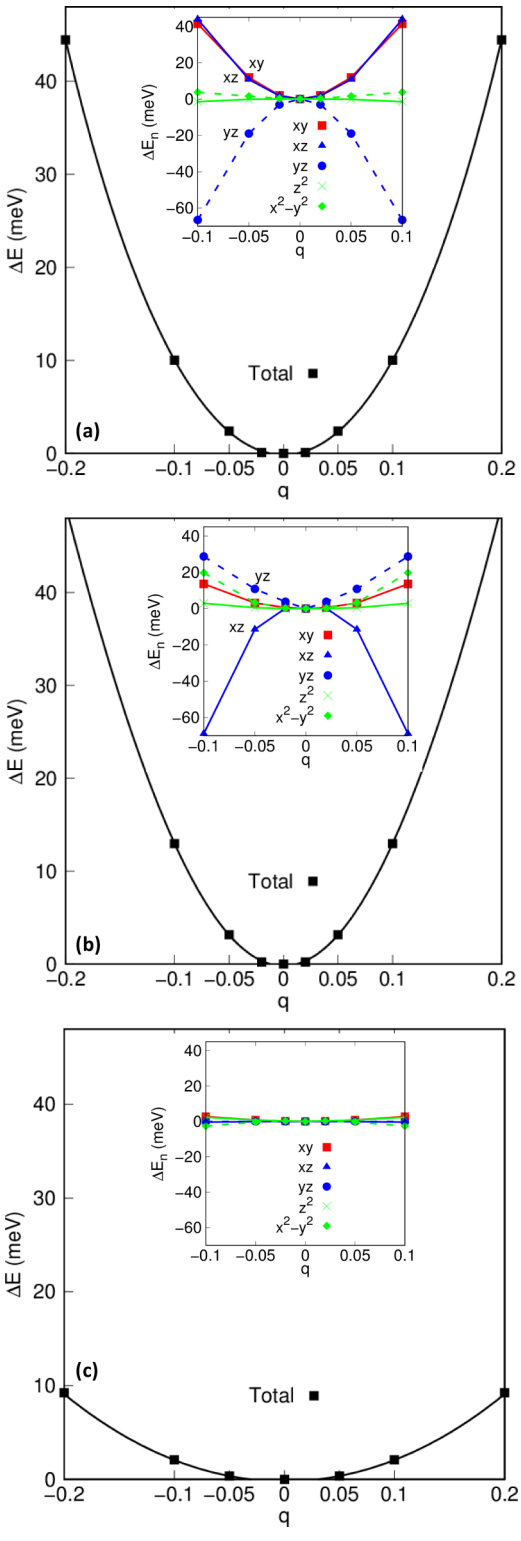

FIG. 2. Frozen magnon energies $\Delta E(q)$ of (a) Fe/MgO, (b) Co/MgO, and (c) Ni/MgO in the absence of electric field ($E_z = 0$), plotted as a function of $q = a/\lambda$, with respect to the ground ferromagnetic states ($q = 0$) as the references. Inset in each panel shows the corresponding orbital energy contributions.

upon the presence of spin canting along the x direction. As will be discussed shortly below, the exchange stiffness mechanism is strongly related to this symmetry breaking. The contributions of the d_{z^2} and $d_{x^2-y^2}$ orbitals to the exchange stiffness are considerably less significant than the other orbitals. Although the O $p_{x,y}$ orbitals at the interface, which hybridize to the Fe $d_{xz,yz}$ orbitals with the π-type hybridization, may give similar contributions, we confirm that the p_x gives a small ferromagnetic energy contribution of 1.1 meV at $q = \pm 0.1$ and the p_y gives a slightly more negative energy contribution of -2.8 meV. Other orbitals are also confirmed to give less significant participation to the exchange stiffness. We note here while these orbital energy contributions may have a dependence on the muffin-tin radii used in the FLAPW calculations, we find that changing the muffin-tin radii does not significantly modify the results. For instance, when the muffin-tin radii of Fe and O are chosen to be 2.15 and 1.35, a.u., respectively, we obtain an exchange stiffness constant of 220 meV Å^2 for the Fe/MgO system at zero field. This number is only slightly shifted from 217.5 meV Å^2 when the muffin-tin radii are chosen to be 2.2 and 1.4 bohrs for Fe and O, respectively. The orbital contributions are practically unchanged. Hence, the conclusion remains valid although different choices of muffin-tin radii are used.

Another interesting feature is obtained by comparing the exchange stiffness of Fe/MgO with those of Co/MgO and Ni/MgO. The $\Delta E(q)$ for Co/MgO is shown in Fig. 2(b) together with the orbital energy contributions in the inset. The general feature of the magnon energy is similar to that of Fe/MgO but the energy dispersion shows a slightly larger slope indicating a stronger exchange stiffness. Indeed, using the polynomial fitting, we obtain an exchange stiffness constant of 296.9 meV Å^2, being larger than that of Fe/MgO by more than 30%. The trend qualitatively follows that in bulk of Fe and Co, inferred from the Bethe-Slater behavior that scales with the number of valence electrons [45,46]. In order to rule out the structural difference, where the Fe-O atomic distance in Fe/MgO (2.17 Å) is shorter than that of Co-O in Co/MgO (2.19 Å), we repeat the calculations for Co/MgO interface using the atomic positions of Fe/MgO. As a result, we obtain only a slightly larger exchange stiffness constant of 304 meV Å^2. The small difference compared to the computed $\mathcal{A}$ of Co/MgO obtained with the relaxed structure implies the crucial role of the difference in the number of the valence electrons between Fe/MgO and Co/MgO. An analysis of the orbital energy contributions moreover reveals a striking difference with that of Fe/MgO. While even in Co/MgO the nature of exchange stiffness involves a strong competition between ferromagnetic and antiferromagnetic contributions, the d_{xz} orbital gives an antiferromagnetic contribution but the d_{yz} prefers a ferromagnetic one, behaving oppositely to those in Fe/MgO. Apart from the d_{z^2} orbital that participates in a very small energy contribution, the behaviors of the other orbitals are almost similar to those of Fe/MgO, although the magnitudes are visibly different.

Additionally, the $\Delta E(q)$ of Ni/MgO shown in Fig. 2(c) shows a smaller slope compared to those of the other two systems. This indicates a weaker exchange stiffness, and indeed, the constant $\mathcal{A}$ is only extracted to be 49.7 meV Å^2. On one hand, the trend follows that of the Bethe-Slater behavior [45,46] reaching the exchange stiffness peak at the Co system.

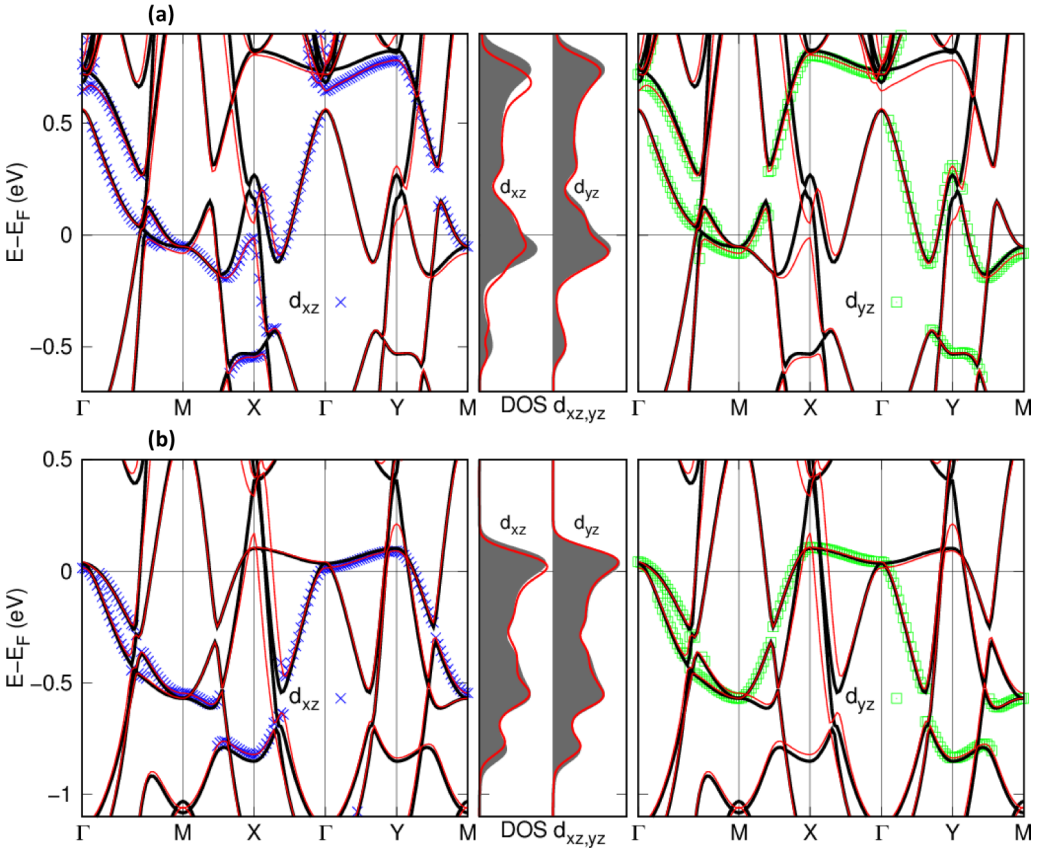

FIG. 3. Band structures and densities of states (DOSs) for minority-spin states of (a) Fe/MgO and (b) Co/MgO interfaces at the absence of applied electric field ($E_z = 0$). The thick (black) and thin (red) lines of the band structures indicate the collinear ferromagnetic state and the spiral state with $q = 0.1$, respectively, while the blue crosses and green squares show the d_{xz} and d_{yz} bands, respectively, at the spiral state. The shaded (gray) curves and solid (red) lines of the DOSs indicate the projected DOSs for the minority-spin states of the collinear ferromagnetic and spiral structures with $q = 0.1$, respectively, to the d_{xz} and d_{yz} orbitals of the transition metal atoms.

On the other hand, the small constant is strongly related to the small magnetic moment of Ni, owing to the extra electron occupying the minority state compared to that of Co. With formally 9 electrons occupying the Ni 3d states, all d bands are almost fully occupied, except for the d_{z^2} orbital which does not practically contribute to the magnetic interaction. For the rest of the paper, therefore, we will only discuss the exchange stiffness of Fe/MgO and Co/MgO systems.

In order to clarify the mechanism in the exchange stiffness, we analyze the band structures and densities of states (DOSs) of the spiral structure with $q = 0.1$ and of the ferromagnetic structure ($q = 0$), as displayed in Fig. 3 for the minority-spin state while the majority-spin bands are almost fully occupied (not shown in figure). The zero energy has been set to the Fermi level. For the Fe/MgO, as shown in Fig. 3(a), two characteristic features in the differences between both magnetic structures can be discerned. First, there are band gap openings in the spin-spiral structure, e.g., at -0.1 eV below the Fermi level at the M point, corresponding to the bonding d_{xz} and d_{yz} states, and at around 0.6 eV above the Fermi level at the Γ point for the antibonding d^*_{xz} and d^*_{yz} ones. Other splittings also appear around the Fermi level at around the X and Y points which behave differently. The band gap opening arises from the breaking of the fourfold symmetry due to the introduction of the spin-spiral rotation along the x direction. The symmetry breaking in the spiral structure is visible from the DOS; in the ferromagnetic state the d_{xz} and d_{yz} bands are degenerate, but in the spiral structure they have different DOS. Second, the bandwidth in the spin-spiral structure becomes narrow since the electron hopping to neighboring atoms, where the spin-up and -down states do not mix, is suppressed due to the spin-spiral rotation. Such effects are more importantly pronounced in the d_{xz} band. In the spin-spiral structure, the degeneracy of the bonding d_{xz} and d_{yz} states below the Fermi level (-0.1 eV) at around the M points is lifted, where the d_{xz} state slightly shifts up to a higher energy compared to that of the d_{yz} state. Additionally, along the Γ-Y direction, the antibonding d^*_{xz} state at about 0.6 eV above the Fermi level shifts down to a lower energy, as also observed in the DOS.

As schematically illustrated in Fig. 4, in the spiral structure the bonding d_{xz} state at around the Fermi level is pushed up in energy but the antibonding d^*_{xz} state shifts down due to the reduction of electron hopping in the spiral structure (t_q) compared to that in the ferromagnetic state (t_0), as mentioned above. Indeed, the calculated occupation number in the d_{xz} orbital decreases by 0.009 electrons on going from the ferromagnetic structure to the spiral structure at $q = 0.1$. For the d_{yz} orbital, in contrast, the behavior is different where the occupation number increases by 0.015 electrons. The energy shift of the d_{xz} state due to the spin-spiral rotation therefore

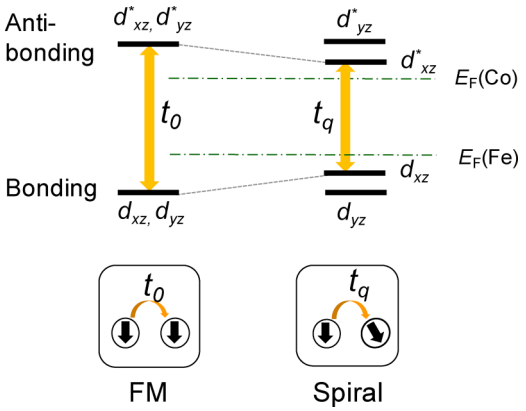

FIG. 4. Schematic energy diagrams of the d_{xz} and d_{yz} states in a collinear ferromagnetic structure (left) and a spin spiral structure (right). A bandwidth narrowing in the d_{xz} band arises from an introduction of the spin spiral rotation along the x direction, where the electron hopping to neighboring atoms is suppressed as illustrated in the insets. The Fermi level is located above the bonding states for Fe/MgO and below the antibonding states for Co/MgO.

transfers the electrons to the bonding d_{yz} state so that the d_{yz} state is getting more occupied. The fact that the charge transfer entering the d_{yz} state is roughly twice compared to that leaving the d_{xz} state indicates that there is another charge transfer to the d_{yz} state. We confirm about 0.008 electrons that move from the d_{xy} state to the d_{yz} state. Such charge transfer promotes the stability of the d_{yz} state while the other two orbitals are becoming energetically less favorable, as demonstrated in Fig. 2(a).

In the Co/MgO, different characteristics can be observed. Due to one more electron occupation compared to that of the Fe/MgO, the DOS [Fig. 3(b)] shows that the Fermi level is located around the antibonding d^*_{xz} and d^*_{yz} states, as schematically shown in Fig. 4. The calculated occupation numbers in the d orbitals at the ferromagnetic structures reflect this fact: while the average occupation in the Fe $d_{xz,yz}$ is 1.18 electrons, that of the Co $d_{xz,yz}$ orbitals is approximately 1.63 electrons. When the spiral structure is introduced, the band gap opening and the bandwidth narrowing take place as in the case of the Fe/MgO. For instance, one can see the band gap openings in the antibonding d^*_{xz} and d^*_{yz} states around the Fermi level at the Γ points and that in the bonding d_{xz} and d_{yz} ones at around -0.6 eV below the Fermi level at the M point. The antibonding d^*_{xz} state further shifts down while the bonding d_{xz} state goes up due to the reduction of the bandwidth, as illustrated in Fig. 4. The energy shift of the d^*_{xz} band around the Fermi level thus increases the stability of the d^*_{xz} antibonding state, which leads to an electron transfer to the d^*_{xz} from the d^*_{yz} states. The present calculation shows that at $q = \pm 0.1$, the d_{yz} occupation of 0.006 electrons moves to the d_{xz} orbital. This explains the exactly opposite behaviors in the orbital energy contributions of the d_{xz} and d_{yz} orbitals to the exchange stiffness compared to those of Fe/MgO, as presented in Fig. 2(b). In Ni/MgO, the changes of d orbital occupations at the different magnetic states are very small, confirming the weak exchange stiffness in this system.

TABLE I. Computed exchange stiffness constant $\mathcal{A}$ (in meV Å^2) and occupation numbers δ of different d orbitals at the collinear ferromagnetic state at zero electric field. Number in parentheses are the corresponding δ at the spin spiral structure with $q = 0.1$.

	Fe/MgO	Co/MgO	Ni/MgO
$\mathcal{A}$	217.5	296.5	49.6
d_{z^2}	1.061 (1.061)	1.064 (1.064)	1.194 (1.193)
d_{xz}	1.180 (1.171)	1.627 (1.642)	1.827 (1.827)
d_{yz}	1.180 (1.195)	1.627 (1.621)	1.827 (1.827)
d_{xy}	1.093 (1.085)	1.166 (1.164)	1.738 (1.737)
$d_{x^2-y^2}$	1.403 (1.402)	1.553 (1.549)	1.595 (1.596)

We note here that while the magnetic exchange stiffness can be explained simply in terms of the population changes (charge transfers) in the d orbitals or the orbital stabilization on going from the ground ferromagnetic states to the spiral structures (see Table I), this approach does not allow us to decompose the magnetic exchange interactions between different types of orbitals. Therefore, the nature of the exchange interactions between different orbitals, for instance the $d_{xz} - d_{xy}$ orbital exchange interaction that was shown to be ferromagnetic in a previous work on bulk Fe due to a double-exchange mechanism [42], cannot be discussed in more detail. Such decomposition would require a careful analysis of the off-diagonal elements of the density matrix, which is beyond the scope of the present paper.

Based on the mechanism we discussed above, we proceed to the effect of applied electric field to exchange stiffness for the Fe/MgO and Co/MgO. The frozen magnon energy in electric fields of ± 5 V/nm and the difference in the orbital energy contributions between both fields are summarized in Fig. 5. We find that the electric field induced atomic displacements at the interfaces play the most important role in the modification of the exchange stiffness for the present TM/MgO systems, where the transition metal (TM) atoms are displaced along the z axis by an application of electric field making a shorter/longer distance with the interface O. The distances between TM and O are altered, from 2.18 Å in the negative electric field to 2.12 Å in the positive one in the case of the Fe/MgO, and from 2.20 Å to 2.18 Å for the Co/MgO. Intuitively, the smaller geometrical modification in the Co/MgO system compared to that of Fe/MgO should lead to smaller electric field effects in the former system. The estimated exchange stiffness constants increase from 212.2 meV Å^2 to 221.6 meV Å^2 in the Fe/MgO and from 293.6 meV Å^2 to 300.0 meV Å^2 in the Co/MgO, on going from negative to positive electric fields. As a direct consequence of the atomic distance modification, the O $2p$–TM $3d$ band hybridization can be expected to alter. However, the most pronounced changes to the projected DOS of the TM $3d$ orbitals take place in the d_{z^2} orbital, due to the σ-type hybridization with the p_z orbital of the oxygen. These occur at the occupied majority-spin states below -1.5 eV and the unoccupied minority-spin states above 1 eV in both systems, not visible within the energy window shown in the DOS in Fig. 6. Nevertheless, these modifications in the DOS of d_{z^2} do not seem to contribute to the exchange stiffness.

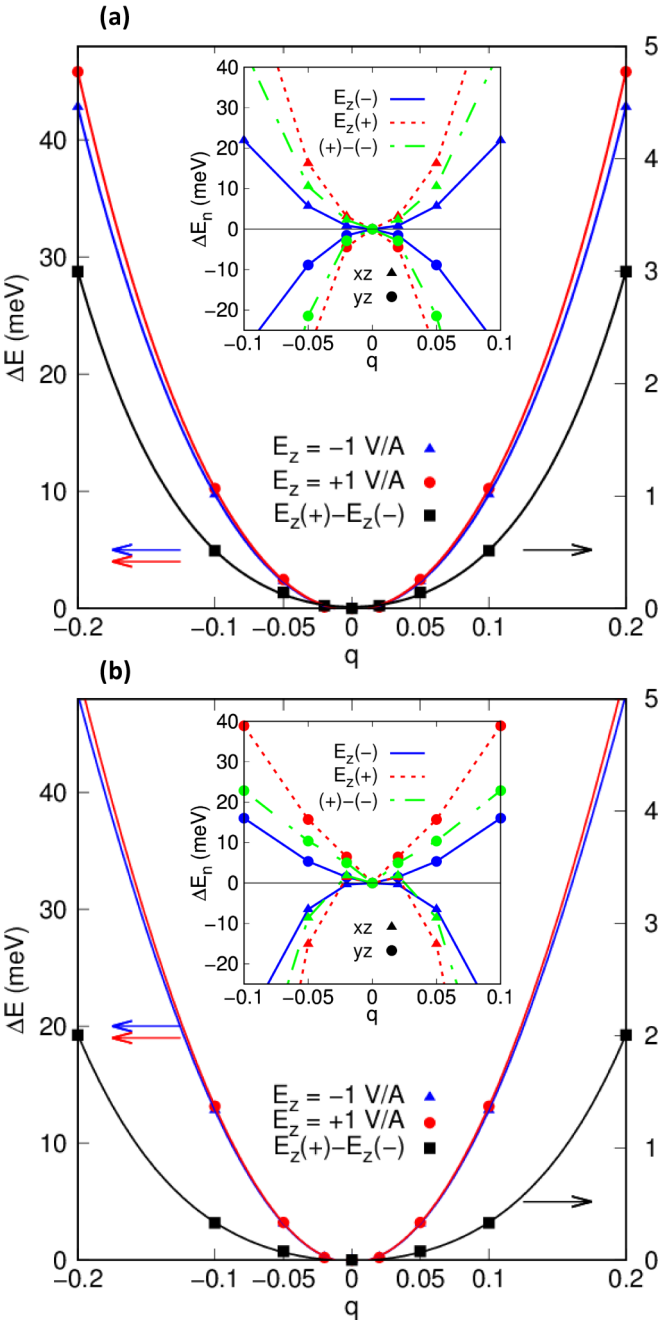

FIG. 5. Frozen magnon energies, $\Delta E(q)$, of (a) Fe/MgO and (b) Co/MgO in applied electric fields ($E_z = \pm 5$ V/nm) as a function of q with respect to the ground ferromagnetic states ($q = 0$) as the references. Red circles (blue triangles) indicate the $\Delta E(q)$ in the positive (negative) field, and the black squares show the difference between positive and negative fields. Inset in each figure shows the corresponding orbital energy contributions of d_{xz} and d_{yz} orbitals to the magnon energy differences, shown using triangles and circles, respectively. Blue (solid) and red (dotted) lines in the insets indicate each contribution in the negative and positive fields, respectively, while the green (dot-dashed) lines indicate the difference between the fields.

Additionally, the d_{xz} and d_{yz} are expected to be pushed above in energy on going from negative to positive fields through the atomic-distance modification. In the ferromagnetic

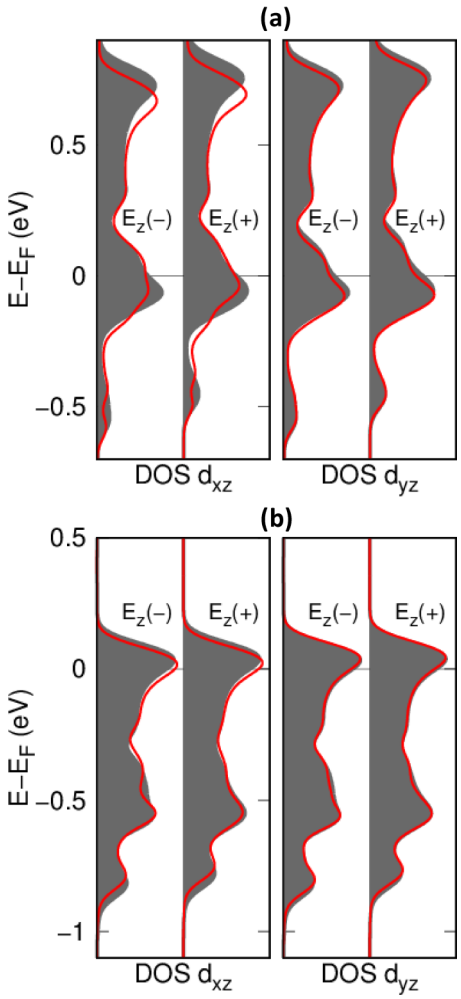

FIG. 6. Densities of states (DOSs) of (a) Fe/MgO and (b) Co/MgO interfaces upon the application of electric field ($E_z = \pm 5$ V/nm). The shaded gray curves and solid red lines indicate the projected DOS for the minority-spin states of the collinear ferromagnetic and magnetic spiral structures with $q = 0.1$, respectively, to the d_{xz} and d_{yz} orbitals of the transition metal atoms for both applied fields; i.e., $E_z(+)$ and $E_z(-)$ denote respectively $E_z = +5$ V/nm and $E_z = -5$ V/nm.

structure, as shown in Fig. 6, the DOSs of the TM atoms in the negative field shift down to a lower energy since the interface TM-O distance increases, while in the positive field these DOSs shift up to a higher energy due to the decrease of the TM-O distance. As a result, for the Fe/MgO, since the bonding d_{xz} and d_{yz} states (e.g., at the M point) in the positive field are closer to the Fermi level compared to that in the negative field, the orbital energy contributions are enhanced at the positive field, as reflected in the inset of Fig. 5. In contrast, for the Co/MgO, since the antibonding d^*_{xz} and d^*_{yz} states in the negative field become closer to the Fermi level (e.g., at the Γ point) than that in the negative field, the orbital energy contributions become less intensified at the negative field. However, these states are almost unaltered by applied fields due to the less sensitivity in the atomic displacements, so one can expect a less significant change in the exchange stiffness.

IV. CONCLUSION

Using first-principles calculations, we have investigated the mechanism of the exchange stiffness in Fe/MgO and Co/MgO interfaces. We demonstrate that there is a competition between positive and negative contributions to the exchange energy favoring the ferromagnetic and antiferromagnetic alignments, respectively, which is determined strongly by the bandwidth and by the position of Fermi level with respect to the d bands. Due to the magnetic spiral structure along the x direction, there is a significant bandwidth narrowing of the d_{xz} band, leading to the breaking of symmetry between the d_{xz} and d_{yz} bands. In the case of Fe/MgO, the Fermi level is situated above the bonding states of d_{xz} and d_{yz} bands, and the narrowing of d_{xz} band decreases the stability of this band upon moving from ferromagnetic states to the spiral structures. On the other hands, since the Fermi level of Co/MgO is below the antibonding d^*_{xz} and d^*_{yz} states, the shift of the d^*_{xz} antibonding state towards a lower energy increases the stability of this orbital, so that it eventually favors antiferromagnetic alignment. When an external electric field is applied, we confirm that the modification of TM-O atomic distances slightly modifies the positions of the bonding and antibonding states of d_{xz} and d_{yz} bands of Fe/MgO and Co/MgO: the bonding states of Fe/MgO shift up closer to the Fermi level on going from negative to positive field, while the antibonding states are pushed down towards the Fermi level on the negative field. The orbital contributions are therefore in both cases enhanced on the positive field.

ACKNOWLEDGMENTS

We thank F. Ando, T. Ono, T. Dohi, S. Kanai, F. Matsukura, and T. Oguchi for fruitful discussions. A.-M.P. was supported by JSPS KAKENHI Grant No. 15H05702. Work was in part supported by JSPS KAKENHI Grant No. 16K05415, and the Cooperative Research Program of Network Joint Research Center for Materials and Devices. Computations were performed at Research Institute for Information Technology, Kyushu University.

[1] S. A. Wolf, D. D. Awschalom, R. A. Buhrman, J. M. Daughton, S. von Molnár, M. L. Roukes, A. Y. Chtchelkanova, and D. M. Treger, Science **294**, 1488 (2001).
[2] C. Chappert, A. Fert, and F. Nguyen Van Dau, Nat. Mater. **6**, 813 (2007).
[3] S. D. Bader and S. S. P. Parkin, Annu. Rev. Condens. Matter. Phys. **1**, 71 (2010).
[4] H. Ohno, Nat. Mater. **9**, 952 (2010).
[5] H. Ohno, D. Chiba, F. Matsukura, T. Omiya, E. Abe, T. Dietl, Y. Ohno, and K. Ohtani, Nature (London) **408**, 944 (2000).
[6] D. Chiba, M. Yamanouchi, F. Matsukura, and H. Ohno, Science **301**, 943 (2003).
[7] M. Weisheit, S. Fähler, A. Marty, Y. Souche, C. Poinsignon, and D. Givord, Science **315**, 349 (2007).
[8] D. Chiba, M. Sawicki, Y. Nishitani, Y. Nakatani, F. Matsukura, and H. Ohno, Nature (London) **455**, 515 (2008).
[9] W.-G. Wang, M. Li, S. Hageman, and C. L. Chien, Nat. Mater. **11**, 64 (2012).
[10] A. J. Schellekens, A. van den Brink, J. H. Franken, H. J. M. Swagten, and B. Koopmans, Nat. Commun. **3**, 847 (2012).
[11] K.-S. Ryu, L. Thomas, S.-H. Yang, and S. Parkin, Nat. Nanotechnol. **8**, 527 (2013).
[12] S. Emori, U. Bauer, S.-M. Ahn, E. Martinez, and G. S. D. Beach, Nat. Mater. **12**, 611 (2013).
[13] F. Ando, H. Kakizakai, T. Koyama, K. Yamada, M. Kawaguchi, S. Kim, K.-J. Kim, T. Moriyama, D. Chiba, and T. Ono, Appl. Phys. Lett. **109**, 022401 (2016).
[14] T. Dohi, S. Kanai, A. Okada, F. Matsukura, and H. Ohno, AIP Adv. **6**, 075017 (2016).
[15] K. Nakamura, R. Shimabukuro, Y. Fujiwara, T. Akiyama, T. Ito, and A. J. Freeman, Phys. Rev. Lett. **102**, 187201 (2009).
[16] M. Endo, S. Kanai, S. Ikeda, F. Matsukura, and H. Ohno, Appl. Phys. Lett. **96**, 212503 (2010).
[17] D. Chiba, S. Fukami, K. Shimamura, N. Ishiwata, K. Kobayashi, and H. Ohno, Nat. Mater. **10**, 853 (2011).
[18] M. Oba, K. Nakamura, T. Akiyama, T. Ito, M. Weinert, and A. J. Freeman, Phys. Rev. Lett. **114**, 107202 (2015).
[19] I. Dzyaloshinskii, J. Chem. Phys. Solids **4**, 241 (1958).
[20] T. Moriya, Phys. Rev. **120**, 91 (1960).
[21] D. A. Smith, J. Magn. Magn. Mater. **1**, 214 (1976).
[22] A. Fert and P. M. Levy, Phys. Rev. Lett. **44**, 1538 (1980).
[23] R. Wiesendanger, Nat. Rev. Mater. **1**, 16044 (2016).
[24] A. L. Sukstanskii and K. Primak, J. Magn. Magn. Mater. **169**, 31 (1997).
[25] B. Schweflinghaus, B. Zimmermann, M. Heide, G. Bihlmayer, and S. Blügel, Phys. Rev. B **94**, 024403 (2016).
[26] G. Chen, T. Ma, A. T. N'Diaye, H. Kwon, C. Won, Y. Wu, and A. K. Schmid, Nat. Commun. **4**, 2671 (2013).
[27] S.-G. Je, D.-H. Kim, S.-C. Yoo, B.-C. Min, K.-J. Lee, and S.-B. Choe, Phys. Rev. B **88**, 214401 (2013).
[28] J.-H. Moon, S.-M. Seo, K.-J. Lee, K.-W. Kim, J. Ryu, H.-W. Lee, R. D. McMichael, and M. D. Stiles, Phys. Rev. B **88**, 184404 (2013).
[29] K. Di, V. L. Zhang, H. S. Lim, S. C. Ng, M. H. Kuok, J. Yu, J. Yoon, X. Qiu, and H. Yang, Phys. Rev. Lett. **114**, 047201 (2015).
[30] J. Cho, N.-H. Kim, S. Lee, J.-S. Kim, R. Lavrijsen, A. Solignac, Y. Yin, D.-S. Han, N. J. J. van Hoof, H. J. M. Swagten *et al.*, Nat. Commun. **6**, 7635 (2015).
[31] J. M. Lee, C. Jang, B.-C. Min, S.-W. Lee, K.-J. Lee, and J. Chang, Nano Lett. **16**, 62 (2016).
[32] J. P. Perdew, K. Burke, and M. Ernzerhof, Phys. Rev. Lett. **77**, 3865 (1996).
[33] E. Wimmer, H. Krakauer, M. Weinert, and A. J. Freeman, Phys. Rev. B **24**, 864 (1981).
[34] M. Weinert, E. Wimmer, and A. J. Freeman, Phys. Rev. B **26**, 4571 (1982).
[35] K. Nakamura, T. Ito, A. J. Freeman, L. Zhong, and J. Fernandez-de-Castro, Phys. Rev. B **67**, 014420 (2003).
[36] C. Herring, in *Magnetism*, edited by G. T. Rado and H. Suhl (Academic Press, New York, 1966).

[37] L. Sandratskii, Adv. Phys. **47**, 91 (1998).
[38] A. Jakobsson, P. Mavropoulos, E. Şaşıoğlu, S. Blügel, M. Ležaić, B. Sanyal, and I. Galanakis, Phys. Rev. B **91**, 174439 (2015).
[39] K. Nakamura, A.-M. Pradipto, T. Akiyama, T. Ito, T. Ono, and M. Weinert (unpublished).
[40] K. Nakamura, N. Mizuno, T. Akiyama, T. Ito, and A. J. Freeman, J. Appl. Phys. **99**, 08N501 (2006).
[41] K. Nakamura, T. Akiyama, T. Ito, and A. J. Freeman, J. Appl. Phys. **105**, 07C304 (2009).
[42] Y. O. Kvashnin, R. Cardias, A. Szilva, I. Di Marco, M. I. Katsnelson, A. I. Lichtenstein, L. Nordström, A. B. Klautau, and O. Eriksson, Phys. Rev. Lett. **116**, 217202 (2016).
[43] J. d'Albuquerque e Castro, D. M. Edwards, J. Mathon, and R. B. Muniz, J. Magn. Magn. Mater. **93**, 295 (1991).
[44] C. A. F. Vaz, J. A. C. Bland, and G. Lauhoff, Rep. Prog. Phys. **71**, 056501 (2008).
[45] J. C. Slater, Phys. Rev. **35**, 509 (1930).
[46] A. Sommerfeld and H. Bethe, in *Handbuch der Physik*, edited by G. Hoppe and K. Scheel (Springer, Berlin, 1933), Vol. 24.